Conventional and inverse magnetocaloric effects in La$_{0.45}$Sr$_{0.55}$MnO$_3$ nanoparticles

A. Rostamnejadi,[1,2,a)] M. Venkatesan,[1] J. Alaria,[1] M. Boese,[3] P. Kameli,[2] H. Salamati,[2] and J. M. D. Coey[1]

[1]*CRANN and School of Physics, Trinity College, Dublin 2, Ireland*
[2]*Department of Physics, Isfahan University of Technology, Isfahan 84156-83111, Iran*
[3]*Advanced Microscopy Laboratory, CRANN, Trinity College, Dublin 2, Ireland*

The magnetocaloric effect of La$_{0.45}$Sr$_{0.55}$MnO$_3$ nanoparticles was studied by dc magnetization measurements. A sample with mean particle size of about 140 nm exhibits both a conventional magnetocaloric effect around the Curie temperature ($\approx$ 295 K) and a large inverse magnetocaloric effect around the antiferromagnetic-ferromagnetic transition temperature ($\approx$ 200 K). The change of magnetic entropy increases monotonically with applied magnetic field and reaches the values of 5.51 J/kg K and -2.35 J/kg K at 200 K and 295 K, respectively, in an applied field of 5 T. The antiferromagnetic-ferromagnetic transition is absent in a 36 nm size sample, which shows only a broad ferromagnetic transition around 340 K and a small change in magnetic entropy near room temperature. The results are discussed in terms of the entropy difference between the A-type antiferromagnetic ground state of La$_{0.45}$Sr$_{0.55}$MnO$_3$ and the low moment ferromagnetic state. By comparing the results obtained on nanoparticles and bulk La$_{0.45}$Sr$_{0.55}$MnO$_3$, one can conclude that the inverse magnetocaloric effect in a material showing the antiferromagnetic-ferromagnetic transition could be improved over a wide range of temperature by tuning the spin disorder in the antiferromagnetic state. © *2011 American Institute of Physics*. [doi:10.1063/1.3614586]

I. INTRODUCTION

The adiabatic application of a magnetic field changes the entropy of a magnetic material.[1–3] The lattice and magnetic parts of the total entropy change compensate each other in the process, so there is a change of temperature of the material with magnetic field, which is known as the magneto-caloric effect (MCE).[1–3] Magnetic refrigeration (MR) based on the MCE has prospects in a future cooling technology. It may be a promising alternative to conventional gas-compression refrigeration, due to its high efficiency and minimal environmental impact.[1–3] Therefore, it is important to find suitable working materials, which offer a large magnetic entropy change in moderate magnetic fields near room temperature, and understand how they function.

Doped perovskite manganites have been a focus of intensive studies since the discovery of colossal magnetoresistance, due to their complex physics and potential applications.[4–6] Manganites are interesting materials for magnetic cooling, due to their ease of preparation, chemical stability, tuneable phase transition temperatures, large magnetic entropy change at moderate magnetic fields, and low cost.[1,3] La$_{1-x}$Sr$_x$MnO$_3$ is one of the most attractive manganites. While its physical properties have been exhaustively studied at low doping levels of strontium (x $<$ 0.5),[4–6] there is less information on the highly doped compositions (x $>$ 0.5)[7–11] and only a few reports on nanoparticle samples.[12,13] La$_{1-x}$Sr$_x$MnO$_3$ with 0.5 $<$ x $<$ 0.6 is a metallic A-type antiferromagnet with a structure of alternating ferromagnetic

(FM) planes at low temperature, but there is a first order transition at about 230 K in single crystals to a FM phase with a Curie point above room temperature.[7–11]

Here, we investigate the MCE by dc magnetization measurements, comparing results for two La$_{0.45}$Sr$_{0.55}$MnO$_3$ nanopowder samples – one with a particle size of 36 nm (S1) and the other with a particle size about 140 nm (S2). The antiferromagnetic (AFM) to FM phase transition at about 230 K, which is first order in the bulk, is absent in S1, and it appears to be a mixture of first order and second order at a lower temperature in S2. The entropy changes and magnetocaloric effects at these transitions are discussed in terms of the effects of particle size and chemical disorder on the A-type AFM ground state and the higher temperature FM state.

II. EXPERIMENTAL RESULTS

Nanoparticles of La$_{0.45}$Sr$_{0.55}$MnO$_3$ (LSMO) were prepared by the sol–gel method.[14] The gel was dried and calcinated at 500 °C for 5 h. The resultant powder was divided into two parts – one part was annealed at 800 °C for 5 h (S1) and the other was annealed at 1000 °C for 5 h and then at 1170 °C for 24 h (S2) to produce a larger particle size. Both samples were characterized by X-ray diffraction (XRD) using Philips X'Pert PRO X-ray diffractometer equipped with a Cu-K$_\alpha$ X-ray source ($\lambda = 1.5406$ Å). The Rietveld refinement, using the FULLPROF program,[15] confirms that they are single phase with no detectable secondary phases. The crystal structure is tetragonal with space group I4/mcm. The X-ray pattern and the Rietveld analysis of the pattern of samples are shown in Fig. 1, and the refined structural

---
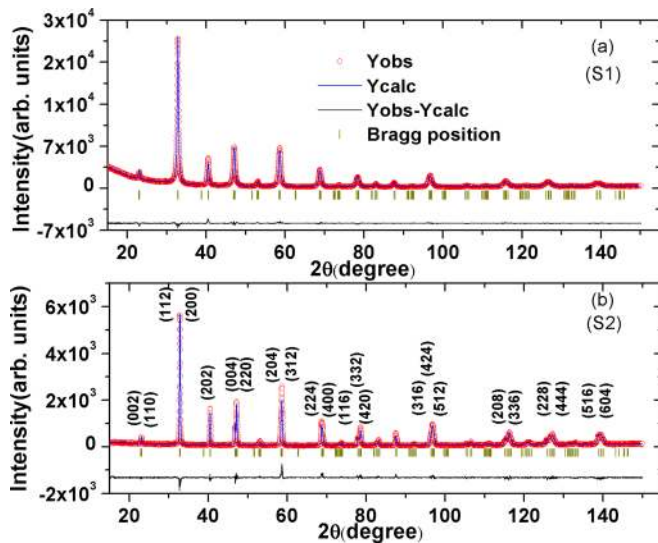a)Author to whom correspondence should be addressed. Electronic mail: ali@ph.iut.ac.ir.

FIG. 1. (Color online) X-ray diffraction pattern and the corresponding Riet-veld refinement for (a) S1 and (b) S2.
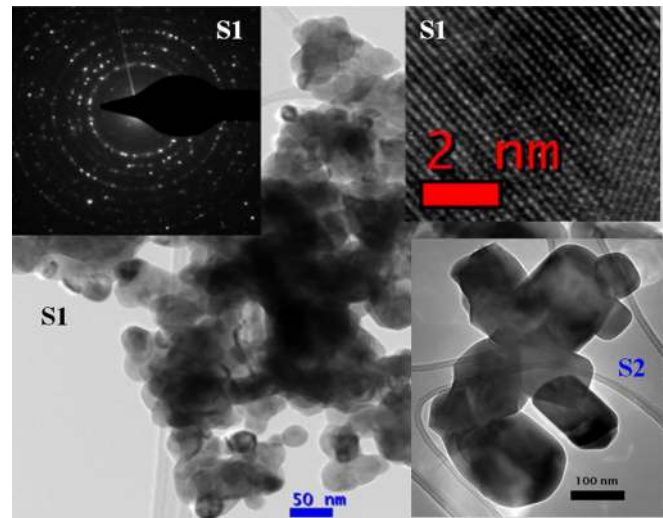

FIG. 2. (Color online) TEM micrograph of S1. Upper panels show the selected area diffraction pattern and HRTEM of S1. TEM micrograph of S2 is shown in lower right hand panel.

parameters are summarized in Table I. A transmission electron microscopy (TEM) micrograph of S1 in Fig. 2 shows that the particle size distribution is monodisperse with a mean value of 36 nm. Most particles have diameter between 32 and 40 nm. The upper panels of Fig. 2 show the high resolution TEM and selected area diffraction pattern of S1. Both confirm the crystalline nature of the sample. The TEM micrograph of S2 is shown in the lower panel of Fig. 2. The particle size ranges between 120–150 nm, with an average size of about 140 nm.

Figure 3 shows the temperature dependence of magnetization, measured in a small field using a Quantum Design MPMS XL SQUID magnetometer in field cooled (FC) mode ($\mu_0 H = 5$ mT). On decreasing temperature, the magnetization of S1 becomes almost temperature-independent and no low temperature transition to an AFM phase takes place. On the other hand, the FC magnetization of S2 drops at temperatures below 230 K, which is due to a progressive transition from FM to A-type AFM. This magnetic phase transition in the bulk $La_{0.45}Sr_{0.55}MnO_3$ is coupled with a sharp transformation from tetragonal to orthorhombic structure.[7,8,10] More detail is given in Figs. 4(a) and 4(b), which show the magnetization curves of both samples as a function of magnetic field at different temperatures. Figure 4(a) shows that the spontaneous magnetization of S1 increases monotonically with decreasing temperature. There is no onset of an AFM phase, although the large high-field slope and small spontaneous moment of just 1.55 μ_B/Mn at 5 K suggest a

randomly-canted FM structure or a structure with a mixed FM + AFM mode. The bulk material exhibits a sharp first order FM $\rightarrow$ AFM transition below 230 K, with little or no FM moment at 5 K in the AFM phase.[7,9] From Fig. 4(b), it can be seen that magnetization of S2 is also unsaturated, even in a magnetic field of 5 T. The magnetization first increases and then decreases with decreasing temperature, which confirms the increasing importance of the AFM mode below 230 K. Our observations are consistent with reports in the literature that the AFM phase transition in the bulk manganites is suppressed with reduction in particle size.[16–20]

In order to check the nature of the magnetic phase transition of the samples, we use the Banerjee criterion.[21,22] According to this criterion, a segment with negative slope in the $\mu_0 H/\sigma$ versus σ^2 curves (Arrott plots) indicates that a magnetic phase transition is first order.[21,22] As can be seen from Figs. 5(a) and 5(b), near the paramagnetic (PM) to FM phase transition, $\mu_0 H/\sigma$ versus σ^2 curves for both samples clearly exhibit positive slope in the entire σ^2 range, which is consistent with second-order transition at the Curie point. The Curie temperatures for S1 and S2 deduced from the Arrott plots are about 340 K and 290 K, respectively. Based on this criterion, the data suggest that the FM to AFM transition in S2 may be a mixture of first order and second order transitions, which is unlike the behavior of bulk of $La_{0.45}Sr_{0.55}MnO_3$, where the transition is clearly first order.[8]

We also measured AC magnetic susceptibility versus temperature on slow cooling and warming. The results show

TABLE I. Summary of the structural parameters extracted from the Rietveld refinement of $La_{0.45}Sr_{0.55}MnO_3$ nanoparticles.

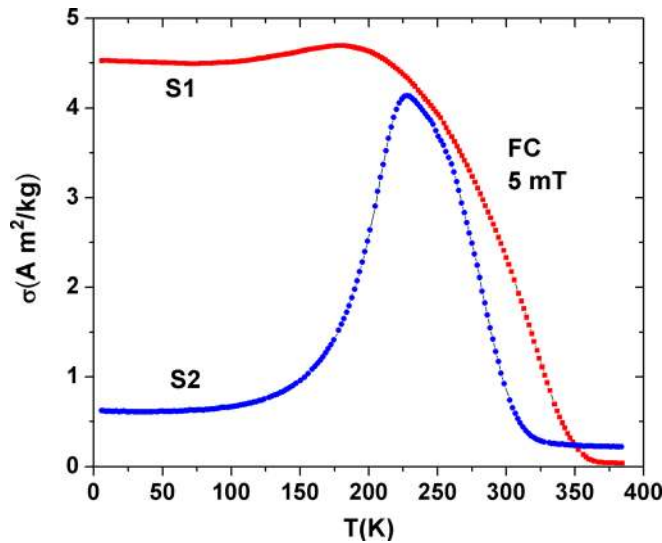| Sample	a (Å)	c (Å)	c/a	$\langle$Mn-O2-Mn$\rangle$ (°)	Mn-O1(Å)	Mn-O2 (Å)	R_P	R_{WP}	R_{Bragg}	χ^2
S1	5.4476(2)	7.7353(4)	1.420	177.70(7)	1.9338(2)	1.9260(6)	4.2	5.54	3.82	2.16
S2	5.4396(2)	7.7494(4)	1.424	169.50(2)	1.9373(6)	1.9310(5)	9.55	12.0	6.56	2.15
Bulk[a]	5.43378(4)	7.7455(1)	1.425	170.85(2)	1.9363(8)	1.9273(5)	5.3	8.37	…	1.282

[a]Reference 7.

FIG. 3. (Color online) Field cooled magnetization of S1 and S2 as a function of temperature at applied field of 5 mT.

the presence of thermal hysteresis of about 7 K around the FM-AFM transition, which indicates the presence of a first order transition. It is difficult to deduce a precise value of the transition temperature because of the residual FM moment at low temperature, but a value of about 203 K can be estimated from the high field slopes. Hueso *et al.*[21] have also reported that the first order magnetic transition in $La_{0.67}Ca_{0.33}MnO_3$ changes to a second order one when the grain size is below 95 nm. The disappearance of AFM phase transition in S1 may be due to the increased importance of surface sites and chemical disorder in $La_{0.45}Sr_{0.55}MnO_3$ nanoparticles, which favor random canting of a FM state at low temperature.[23]

The magnetic entropy changes rapidly near a phase transition, where the magnetization changes rapidly.[1–3] Therefore, a large magnetocaloric effect is expected in the vicinity of Curie temperature. It is less clear why the entropy should vary at the FM-AFM transition in $La_{0.45}Sr_{0.55}MnO_3$, where the magnitude of the manganese moment could be conserved as the magnetic order changes. We address this point in the discussion.

Usually, two basic parameters, magnetic entropy change (ΔS_M) and adiabatic temperature change (ΔT_{ad}), are used to characterize the magnetocaloric effect.[1–3,8] Based on thermodynamic theory, the isothermal magnetic entropy change associated with magnetic field variation from zero to H is given by[1]

$$\Delta S_M = S_M(T,H) - S_M(T,0) = \int_0^H \left(\frac{\partial S_M(T,H')}{\partial H'} \right)_T dH'. \quad (1)$$

The magnetic entropy is related to the magnetization M, magnetic field strength H, and absolute temperature T through the Maxwell relation

$$\left(\frac{\partial S_M(T,H)}{\partial \mu_0 H} \right)_T = \left(\frac{\partial M(T,H)}{\partial T} \right)_H. \quad (2)$$

In the case of magnetization measurements at small discrete magnetic field and temperature intervals, ΔS_M can be approximated to
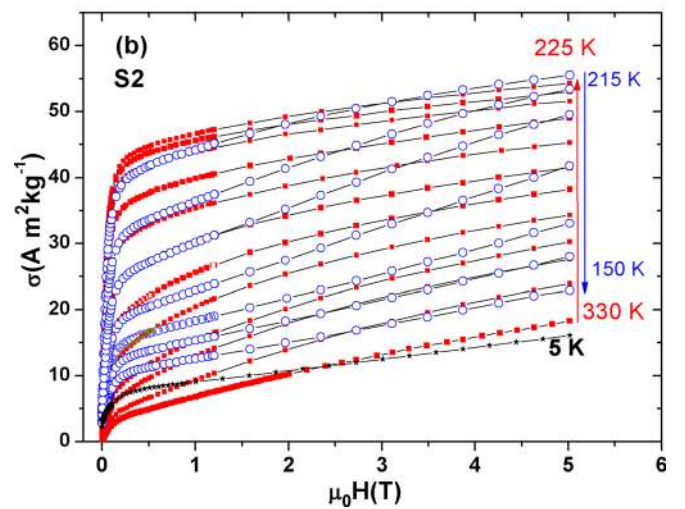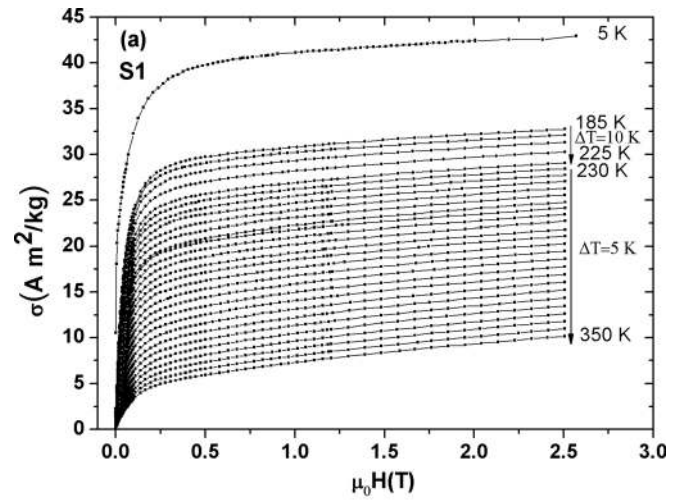

FIG. 4. (Color online) Magnetic field dependence of magnetization at different temperatures for (a) S1 and (b) S2.

$$\Delta S_M(T,H) = \frac{\mu_0}{\Delta T} \left[\int_0^H M(T+\Delta T, H')dH' - \int_0^H M(T,H')dH' \right]. \quad (3)$$

Figure 6(a) shows the magnetic entropy change of S1 as a function of temperature for $\Delta \mu_0 H = 2.5$ T. It can be seen that ΔS_M is negative in the entire temperature range and its magnitude is -0.45 J/kg K at room temperature. Figure 6(b) shows the magnetic entropy change of S2 versus temperature in different applied magnetic fields deduced in the same way. As expected, the magnitude of the entropy change is large around the PM-FM (295 K) and FM-AFM (200 K) transition temperatures and shows strong magnetic field dependence. The value of ΔS_M around Curie temperature is negative, but in contrast, its value around FM-AFM phase transition is positive. Such an effect with a positive sign of ΔS_M is known as the inverse magnetocaloric effect.[24–26] It has been reported in various other magnetic materials, such as $La_{0.125}Ca_{0.875}MnO_3$,[24] Heusler alloys,[25–27] $CeFe_2$ and Ru-doped $CeFe_2$ alloys,[28] $Pr_{0.68}Ca_{0.32}MnO_3$,[29] $Pr_{0.95}Ag_{0.05}MnO_3$,[30] and $Pr_{0.5}Sr_{0.5}MnO_3$.[31] Such a material cools adiabatically when a magnetic field is applied and could be used as a sink for heat generated by conventional
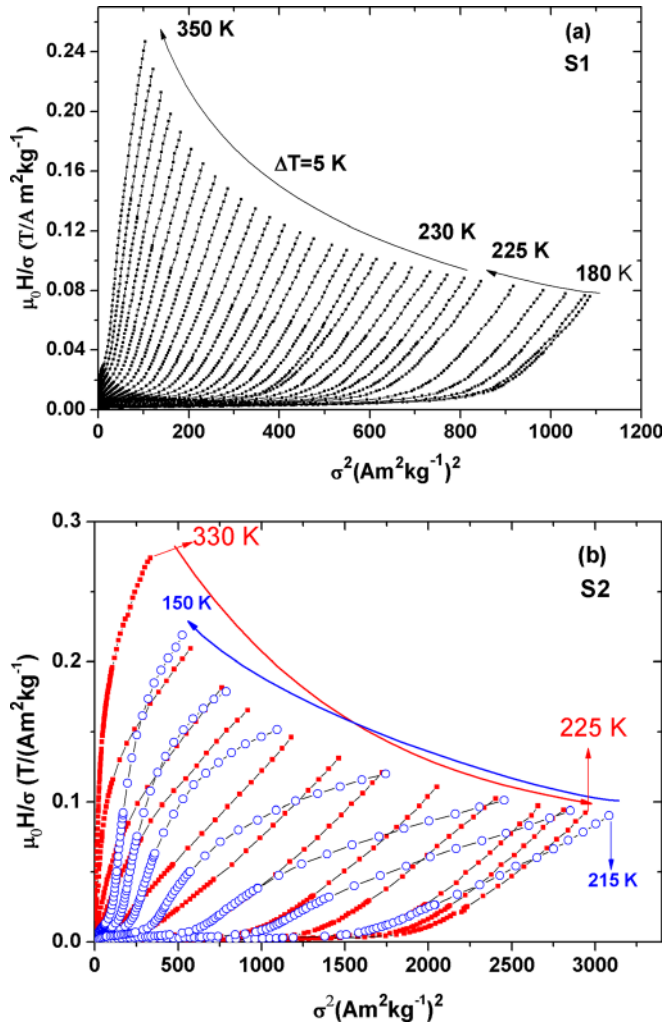
FIG. 5. (Color online) Arrott plot ($\mu_0 H/\sigma$ vs σ^2) at different temperatures for (a) S1 and (b) S2.
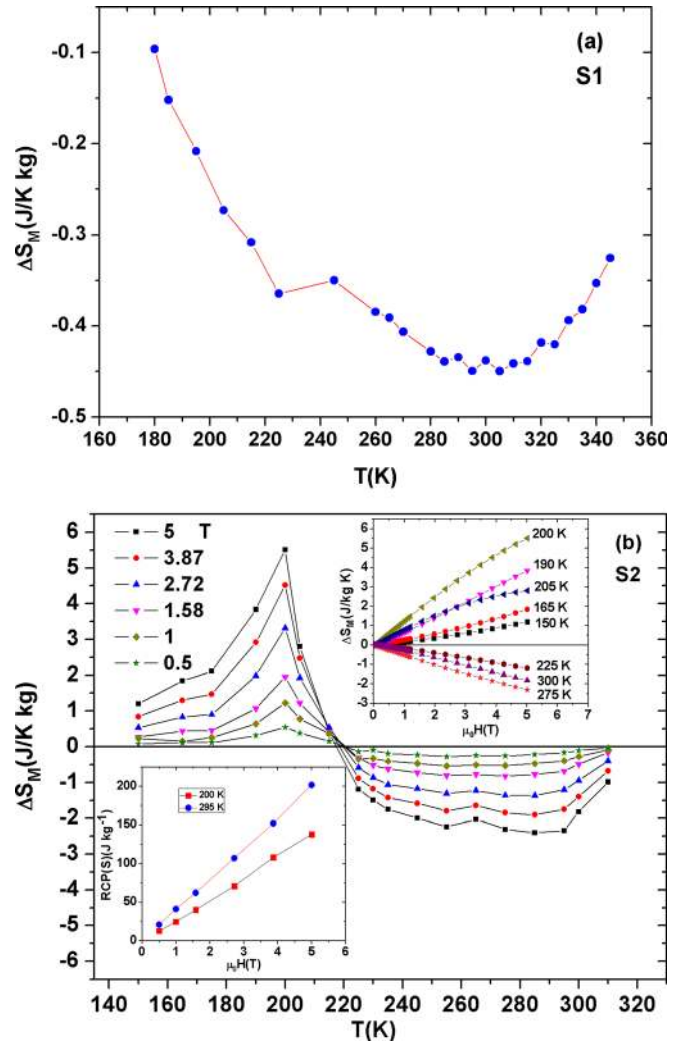

FIG. 6. (Color online) Magnetic entropy change vs temperature for (a) S1 for magnetic field change from zero to 2.5 T and (b) S2 at different magnetic fields. Lower inset of (b) shows the values of RCP(S) vs magnetic field, and upper inset shows the field dependence of magnetic entropy change at different temperatures.

MCE materials.[24–26] Therefore, inverse MCE materials can increase the refrigeration efficiency when coupled with a conventional MCE material.[24–26] From Fig. 6(b), the normal magnetic entropy change of S2 extends over a wide range of temperature around the Curie temperature, which is useful for room temperature magnetic refrigeration. ΔS_M ranges from -0.17 to -2.35 J kg^{-1} K^{-1}, corresponding to applied magnetic fields ranging from 0.5 to 5 T at 295 K. As can be noted from Fig. 6(b), the positive magnetic entropy change reaches its highest values, ranging from 0.54 to 5.51 J kg^{-1} K^{-1} for field variations ranging from 0.5 to 5 T at 200 K. The maximum value of ΔS_M of S2 at 295 and 200 K is about 23% and 54% of that of Gd (10.2 J kg^{-1} K^{-1} for $\Delta\mu_0 H = 5$ T at 294 K), respectively.[3]

The adiabatic temperature change, ΔT_{ad}, can be calculated as[1]

$$\Delta T_{ad} = -\mu_0 \int_0^H \left(\frac{T}{C_P(T,H')}\right)\left(\frac{\partial M(T,H')}{\partial T}\right)_{H'} dH', \quad (4)$$

where $C_P(T, H)$ is the heat capacity. Using expressions (1) and (3), ΔT_{ad} can be estimated as[1]

$$\Delta T_{ad}(T,H) = -\Delta S_M(T,H)\left(\frac{T}{C_P(T,H)}\right). \quad (5)$$

The adiabatic temperature change depends on temperature, heat capacity, and magnetic entropy change, as shown by Eq. (5). We have estimated the adiabatic temperature change of S2 from Eq. (5), using $C_P \approx 520$ and 525 J kg^{-1} K^{-1} at 295 K and $C_P \approx 450$ and 430 J kg^{-1} K^{-1} at 200 K for bulk La$_{0.45}$Sr$_{0.55}$MnO$_3$, at magnetic fields of 1 T and 5 T, respectively.[8] The values $\Delta T_{ad} \sim -0.6$ K and -2.6 K at 200 K and $\Delta T_{ad} \sim 0.2$ K and 1.3 K at 295 K are obtained for $\Delta\mu_0 H = 1$ and 5 T, respectively.

The relative cooling power (RCP(S)) is another important parameter used to evaluate the cooling efficiency of magnetic refrigerants; it is defined as[3]

$$RCP(S) = -\Delta S_M(T,H) \times \delta T_{FWHM}, \quad (6)$$

Where δT_{FWHM} is the full width at half maximum of the magnetic entropy change curve. This parameter corresponds to the amount of heat that can be transferred between the

cold and hot parts of the refrigerator in one ideal thermodynamic cycle. In general, the better the RCP for a given magnetic field, the better the material is for magnetic refrigeration. The lower inset of Fig. 6(b) shows the absolute value of RCP for S2 versus applied field at 295 K and 200 K. It can be seen from the lower inset of Fig. 6(b) that RCP increases monotonically as the field increases and reaches the values of 138 J kg^{-1} and 201 J kg^{-1} for $\Delta\mu_0 H = 5$ T at 200 K and 295 K, respectively, which are about 33% and 49% of that of Gd.[3] These values are comparable to those reported for other manganites.[3] However, due to the partly first order nature of the transition, there may be correction from hysteresis loss that must be considered when calculating the RCP of magnetic materials subjected to field cycling.[31,32] The contribution of hysteresis losses in RCP, determined from the thermal hysteresis of ac magnetic susceptibility, is about 38 J kg^{-1} for $\Delta\mu_0 H = 5$ T. To evaluate the applicability of La$_{0.45}$Sr$_{0.55}$MnO$_3$ nanoparticles as a magnetic refrigerant, the obtained values of ΔS_M in our study are compared in Table II with those reported in the literature for several other nanoparticles of magnetic materials.[21,24,32–37]

III. DISCUSSION

First, we discuss the origin of the FM phase and the disappearance of the FM-AFM phase transition in our nanoparticle S1 sample. Several experimental reports show that charge-ordered (CO) AFM manganites behave differently in the bulk and in nanoparticle form.[16–20,38,39] For example, the CO state is suppressed and partly FM states have been reported,[17–20,38,39] which exhibit a reduced Mn moment,[17–20,38,39] but in some cases, the moment approaches the full spin-only value.[20] The mechanism of FM phase formation and the effect of particle size on the magnetic properties is still a topic for debate, but several scenarios have been proposed, as are shown in Fig. 7. In nanoparticles, the surface/volume ratio is large and the surface influences both magnetic and electronic properties. Electron interactions modify the competing double exchange (DE) and super exchange (SE) interactions at the surface of particles.

The first scenario is based on a core-shell model, where a nanoparticle is composed of a FM or partly FM shell with an AFM core whose size decreases with decreasing particle size (Fig. 7(a)).[16,18,40,41] The uncompensated AFM spins at the surface change the collinear AFM configuration. A recent theoretical study suggesting surface phase separation with a FM tendency at the surface of CO manganites[41] indicates that the increase in charge density due to the unscreened

Coulomb interactions changes the surface layer from an AFM/CO to a phase-separated electronic state with a FM tendency in the surface shell. It yields a weak FM fraction of about 40% in the shell, while the inner core is still in stable charge ordered AFM state. This study is consistent with some experimental reports, which show weak FM fraction (a few percent) in the AFM ground state.[41] However, there are some reports which show relatively strong FM fraction in nanosized manganites, which cannot be described by purely surface magnetism. For example, the FM fraction in Nd$_{0.5}$Ca$_{0.5}$MnO$_3$ nanoparticles (20 nm) is about 30% at 10 K,[17] in La$_{0.4}$Ca$_{0.6}$MnO$_3$ nanoparticles (20 and 60 nm) is 30% at 3 K,[18] in La$_{0.5}$Ca$_{0.5}$MnO$_3$ nanoparticles (25 nm) is 40% at 5 K,[19] in La$_{0.5}$Ca$_{0.5}$MnO$_3$ nanoparticles (15 nm) is 91% at 10 K,[20] and in Ca$_{0.82}$La$_{0.18}$MnO$_3$ nanoparticles (20–30 nm) is about 22% at 5 K.[39] In our case, from extrapolation of magnetization to zero field, the FM fraction of S1 and S2 are about 45% and 8%, respectively, at 5 K. This suggests a second scenario, where the core is FM without charge order and the shell has disordered frozen spins (Fig. 7(b)).[19] DE is active in the core, where there is no charge order, but electrons are localized in the shell, which may be positively charged, leading to competing frustrated FM and AFM interactions.

A third scenario is based on the surface hydrostatic pressure, due to the size effects in nanosized manganites.[20] The surface pressure changes the crystal structure, destabilizes charge ordering, and enhances the ferromagnetism.[20] Recently, Wang and Fan proposed a description based on the analysis of the crystal structure in nanowires and nanoparticles of Ca$_{0.82}$La$_{0.18}$MnO$_3$. They suggested that the nanodimensional or surface effect is not the reason for suppressing charge ordering and developing ferromagnetism, but intrinsic structural distortions suppress the CO state and develop the FM state.[39] Furthermore, Jirák *et al.*[19] found little influence of particle size on crystal structure.

While most studies are focused on half-doped and electron-doped CO AFM manganites, there is not a systematic study of magnetic properties of La$_{1-x}$Sr$_x$MnO$_3$ nanoparticles for $x > 0.5$. We can describe our results in terms of competing double DE and SE interactions. The DE interaction mediate FM coupling between Mn^{3+} and Mn^{4+} ions within the *ab* plane, and the SE interaction mediate out of plane AFM coupling along the *c* axis.[8,9,11,24] As can be seen from Table I, the lattice constant along the *c* axis and the Mn-O1 bond length of S1 are decreased and the Mn-O2-Mn bond angle is increased toward 180°, while these parameters for S2 are almost the same as those for the bulk. This suggests that, in S1, the DE interaction could dominate the SE interaction and ferromagnetism becomes more favorable both within the *ab* plane and along the *c* axis. However, local chemical inhomogeneity may induce internal strain inside the nanoparticles. Furthermore, the conduction electrons tend to be localized at the surface of particles because of band narrowing and the possibility of unconstrained Jahn-Teller distortion for the Mn^{3+}. According to the third scenario, the local strain and surface pressure due to size effect can locally change the competition between DE and SE interactions in LSMO nanoparticles. Therefore, the A-type
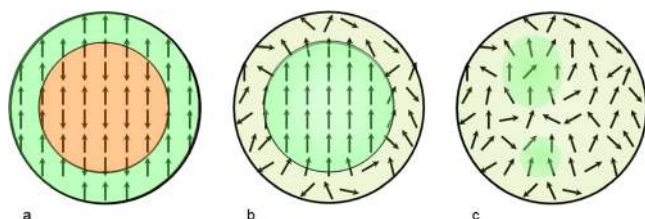

FIG. 7. (Color online) Model magnetic structures for AFM nanoparticles. a) AFM core, FM shell. b) FM core, canted shell. c) FM clusters embedded in a canted structure.

AFM ground state may change to a randomly canted FM state, which leads to disappearance of FM-AFM phase trantion.[23] Our observations suggest that, in addition to surface FM tendency, FM clusters might also exist in the whole volume of LSMO nanoparticles (Fig. 7(c)).

We now discuss the magnetocaloric effect in LSMO nanoparticles. The spin-only moment for the manganese in $La_{0.45}Sr_{0.55}MnO_3$ is 3.45 μ_B/Mn. In a neutron diffraction study, the ordered AFM moment in the AFM mode was found to be 2.82 μ_B/Mn at 12 K.[7] The discrepancy might be attributed to zero-point spin deviation and hybridization of the manganese orbitals in adjacent planes. However, the magnetic moment in the FM phase, above 220 K, is very much smaller. The spin-only FM moment is encountered in this manganite system in the composition range of $0.1 < x < 0.5$.[4–9] Moments reported in the literature for $x = 0.55$ are around 2.0 μ_B/Mn in 5 T, but there is a large high-field slope, which extrapolates to 1.8 μ_B/Mn in zero field.[7–9] In our case, the FM moment is even lower; 1.75 μ_B/Mn for S1 in 5 T at 5 K, extrapolating to 1.55 μ_B/Mn in zero field and 1.85 μ_B/Mn for S2 in 5 T at 200 K, extrapolating to 1.0 μ_B/Mn in zero field. There is plenty of disorder of the moments in the "FM" phase.

What is the nature of the disorder? The first-order transition observed in single crystals is accompanied by a latent heat, corresponding to an entropy change of 1.0 ± 0.1 J mol^{-1} K^{-1}. The magnetic field dependence of the transition temperature gives a similar value for the entropy change at the transition. The transition is magnetically driven, and the magnetization drags the structural transformation along.[8] A much larger entropy, of order R(ln 3.82 – ln 2.0) = 5.4 J mol^{-1}K^{-1}, and a narrow range of temperature, where the FM phase is stable, would be anticipated if the transverse spin components became fully disordered at the first-order transition. In fact, there must be frozen transverse spin components, either short-range

AFM order or random spin canting, which produce no net magnetization.

The normal and inverse magnetocaloric effects in $La_{0.45}Sr_{0.55}MnO_3$ follow because the magnetic entropy of the FM state is intermediate between that of the AFM state (~ 0 J mol^{-1} K^{-1}) and the fully disordered PM state (11.1 J mol^{-1} K^{-1}). Adiabatic application of a magnetic field just above T_C therefore decreases the magnetic entropy by inducing order in the PM phase, which leads to an increase of temperature. However, applying a magnetic field just below the first-order transition stabilizes the FM phase, which has greater entropy than the AFM ground state, thereby reducing the temperature.

In our sample S2, the AFM-FM transition is extended in temperature and is mainly second order in character. The changes of entropy and temperature, which we infer in 5 T (1.23 J mol^{-1} K and -2.6 K), are substantially greater than the values reported for a bulk sample with a clear first-order transition in 7 T (0.73 J mol^{-1} K and -1.5 K).[8] We associate the difference with the lower FM moment in S2 and greater magnetic entropy associated with the transverse spin components in the FM phase. A consequence is a lesser entropy change and a smaller magnetocaloric effect at the Curie temperature. The entropy change in S2 is comparable to that of bulk $La_{0.125}Ca_{0.875}MnO_3$ (~ 6.1 J kg^{-1} K^{-1} for $\Delta\mu_0 H = 7$ T).[24] In addition, the effect is much greater than that of nanocrystalline $La_{0.125}Ca_{0.875}MnO_3$ near the AFM-FM transition temperature.[24]

The orthorhombic, AFM phase of bulk $La_{0.45}Sr_{0.55}MnO_3$ is metallic, like the tetragonal FM phase.[8,42] There can be no charge order and, therefore, no contribution to the entropy of the AFM-FM transition on this account; however, destruction of $x^2 - y^2$ orbital order at the transition could make a contribution to the entropy of up to 0.45 R ln 2 = 2.6 J mol^{-1} K^{-1} for localized electrons. This must be greatly attenuated in the metallic state.

TABLE II. Summary of magnetocaloric properties of $La_{0.45}Sr_{0.55}MnO_3$ nanoparticles compared with other magnetic nanoparticles.

Composition	Size (nm)	T_{max}(K)	$\mu_0\Delta H$(T)	ΔS_M(J/kg K)	RCP(S) (J/kg)	Reference
$La_{0.67}Ca_{0.33}Mn_{0.9}V_{0.1}O_3$	39	253.5	5	-4.6	135	33
DyCo	15–50	7.5	6	-13.2	…	34
$Pr_{0.65}(Ca_{0.7}Sr_{0.3})_{0.35}MnO_3$	67	220	5	-6	…	35
$Pr_{0.65}(Ca_{0.7}Sr_{0.3})_{0.35}MnO_3$	52	220	5	-3.5	…	35
$La_{0.125}Ca_{0.875}MnO_3$	70	~ 110	7	~ 1.4	…	24
$La_{0.125}Ca_{0.875}MnO_3$	50	~ 120	7	~ 0.1	…	24
$CoFe_2O_4$	13	213	1.3	0.23	…	36
$La_{0.67}Sr_{0.33}MnO_3$	85	369	1.5	-1.74	52.2	37
$La_{0.67}Sr_{0.33}MnO_3$	51	367	1.5	-1.3	48.1	37
$La_{0.67}Sr_{0.33}MnO_3$	32	362	1.5	-0.32	20.48	37
$La_{0.67}Ca_{0.33}MnO_{3-\delta}$	60	~ 225	1	$\sim (1.75)$	…	21
$La_{0.67}Ca_{0.33}MnO_{3-\delta}$	500	~ 265	1	$\sim (-5)$	…	21
$La_{0.45}Sr_{0.55}MnO_3$	36	295	2.5	0.45	65	This work
$La_{0.45}Sr_{0.55}MnO_3$	~ 140	295	5	-2.35	201	This work
$La_{0.45}Sr_{0.55}MnO_3$	~ 140	200	5	5.51	138	This work
$La_{0.45}Sr_{0.55}MnO_3$	~ 140	295	1	-0.4	41	This work
$La_{0.45}Sr_{0.55}MnO_3$	~ 140	200	1	1.23	25	This work
$La_{0.35}Pr_{0.275}Ca_{0.375}MnO_3$	50	215	5	6.2	225.6	32
$La_{0.35}Pr_{0.275}Ca_{0.375}MnO_3$	50	215	1	2.94	37.2	32

Manganite nanoparticles exhibit magnetic properties which are different from the bulk material. In $La_{0.45}Sr_{0.55}MnO_3$, the sharp FM-AFM transition is broadened and then suppressed entirely as the particle size decreases. The lattice contracts slightly in the nanoparticles, and the Mn-O2-Mn angle increases toward $180°$, which will modify the balance of double exchange and superexchange interactions. Furthermore, conduction electrons in metallic mixed-valence manganites tend to be localized at the surface because of band narrowing and the possibility of unconstrained Jahn-Teller distortion for the Mn^{3+}. This reduces the FM interactions in a surface shell and may lead to random spin canting in a surface layer:[23] the second scenario. The effect of these changes is to stabilize the low-moment ferromagnet relative to the A-type antiferromagnet, regardless of magnetic entropy.

IV. CONCLUSIONS

Structural and surface effects destabilize the A-type antiferromagnet in the smaller 36 nm $La_{0.45}Sr_{0.55}MnO_3$ nanoparticles, but their effect in larger 140 nm particles is to increase the entropy of the FM phase compared to that of the bulk material and to broaden the FM-AFM transition. As a result, the inverse magnetocaloric effect is enhanced, while it may be possible to shift the FM-AFM transition to higher temperatures by a combination of further chemical substitution, control of particle size, and surface treatment; this is likely to entail a smaller entropy change at the magnetically driven FM-FM transition. Nevertheless, the controllable normal and inverse magnetocaloric effects in these nanoparticles in extended temperature ranges may open the prospect of novel applications in magnetic refrigeration.

ACKNOWLEDGMENTS

[1] A. M. Tishin and I. Spichkin, *The Magnetocaloric Effect and Its Applications* (Institute of Physics, Bristol, 2003).
[2] K. A. Gschneidner, V. K. Pecharsky, and A. O. Tsokol, Rep. Prog. Phys. **68**, 1479 (2005).
[3] M. H. Phan and S. C. Yu, J. Magn. Magn. Mater. **308**, 325 (2007).
[4] J. M. D. Coey, M. Viret, and S. Von Molnar, Adv. Phys. **58**, 571 (2009).
[5] E. Dagotto, *Nanoscale Phase Separation and Colossal Magnetoresistance* (Springer-Verlag, Berlin, 2002).
[6] M. B. Salamon and M. Jaime, Rev. Mod. Phys. **73**, 583 (2001).
[7] O. Chmaissem, B. Dabrowski, S. Kolesnik, J. Mais, J. D. Jorgensen, and S. Short, Phys. Rev. B **67**, 094431 (2003).
[8] A. Szewczyk, M. Gutowska, and B. Dabrowski, Phys. Rev. B **72**, 224429 (2005).
[9] J. Hemberger, A. Krimmel, T. Kurz, H. A. Krug von Nidda, V. Y. Ivanov, A. A. Mukhin, A. M. Balbashov, and A. Loidl, Phys. Rev. B **66**, 094410 (2002).
[10] Y. Moritomo, T. Akimoto, A. Nakamura, K. Ohoyama, and M. Ohashi, Phys. Rev. B **58**, 5544 (1998).
[11] J. Dho, W. S. Kim, and N. H. Hur, Phys. Rev. Lett. **87**, 187201 (2001).
[12] Y. Tian, D. Chen, and X. Jiao, Chem. Mater. **18**, 6088 (2006).
[13] X. Zhu, H. Lei, S. Zhang, X. Zhu, B. Wang, G. Li, X. Luo, W. Song, J. Dai, Y. Sun, D. Shi, and S. Dou, J. Magn. Magn. Mater. **321**, 2009 (2009).
[14] A. Rostamnejadi, H. Salamati, P. Kameli, and H. Ahmadvand, J. Magn. Magn. Mater. **321**, 3126 (2009).
[15] J. Rodríguez-Carvajal, Physica B **192**, 55 (1993).
[16] T. Zhang and M. Dressel, Phys. Rev. B **80**, 014435 (2009).
[17] S. S. Rao, S. Tripathi, D. Pandey, and S. V. Bhat, Phys. Rev. B **74**, 144416 (2006).
[18] C. L. Lu, S. Dong, K. F. Wang, F. Gao, P. L. Li, L. Y. Lv, and J. M. Liu, Appl. Phys. Lett. **91**, 032502 (2007).
[19] Z. Jirák, E. Hadová, O. Kaman, K. Knížek, M. Maryško, E. Pollert, M. Dlouhá, and S. Vratislav, Phys. Rev. B **81**, 024403 (2010).
[20] T. Sarkar, B. Ghosh, A. K. Raychaudhuri, and T. Chatterji, Phys. Rev. B **77**, 235112 (2008).
[21] L. E. Hueso, P. Sande, D. R. Miguéns, J. Rivas, F. Rivadulla, and M. A. López-Quintela, J. Appl. Phys. **91**, 9943 (2002).
[22] J. Mira, J. Rivas, F. Rivadulla, C. Vázquez–Vázquez, and M. A. López-Quintela, Phys. Rev. B **60**, 2998 (1999).
[23] J. M. D. Coey, Can. J. Phys. **65**, 1210 (1987).
[24] A. Biswas, T. Samanta, S. Banerjee, and I. Das, Appl. Phys. Lett. **94**, 233109 (2009).
[25] T. Krenke, E. Duman, M. Acet, E. F. Wassermann, X. Moya, L. Mañosa, and A. Planes, Nature Mater. **4**, 450 (2005).
[26] A. K. Nayak, K. G. Suresh, and A. K. Nigam, J. Phys. D: Appl. Phys. **42**, 035009 (2009).
[27] D. Bourgault, J. Tillier, P. Courtois, D. Maillard, and X. Chaud, Appl. Phys. Lett. **96**, 132501 (2010).
[28] M. K. Chattopadhyay, M. A. Manekar, and S. B. Roy, J. Phys. D: Appl. Phys. **39**, 1006 (2006).
[29] A. M. Gomes, F. Garcia, A. P. Guimarães, M. S. Reis, and V. S. Amaral, Appl. Phys. Lett. **85**, 4974 (2004).
[30] A. Gamzatov, A. Batdalov, A. Aliev, L. Khanov, H. Ahmadvand, H. Salamati, and P. Kameli, JETP Lett. **91**, 341 (2010).
[31] N. S. Bingham, M. H. Phan, H. Srikanth, M. A. Torija, and C. Leighton, J. Appl. Phys. **106**, 023909 (2009).
[32] M. H. Phan, S. Chandra, N. S. Bingham, H. Srikanth, C. L. Zhang, S. W. Cheong, T. D. Hoang, and H. D. Chinh, Appl. Phys. Lett. **97**, 242506 (2010).
[33] P. Nisha, S. S. Pillai, A. Darbandi, A. Misra, K. G. Suresh, M. R. Varma, and H. Hahn, J. Phys. D: Appl. Phys. **43**, 135001 (2010).
[34] S. Ma, W. B. Cui, D. Li, N. K. Sun, D. Y. Geng, X. Jiang, and Z. D. Zhang, Appl. Phys. Lett. **92**, 173113 (2008).
[35] A. Biswas, T. Samanta, S. Banerjee, and I. Das, Appl. Phys. Lett. **92**, 212502 (2008).
[36] E. V. Gopalan, I. A. Al-Omari, D. S. Kumar, Y. Yoshida, P. A. Joy, and M. R. Anantharaman, Appl. Phys. A **99**, 497 (2010).
[37] W. J. Lu, X. Luo, C. Y. Hao, W. H. Song, and Y. P. Sun, J. Appl. Phys. **104**, 113908 (2008).
[38] S. Rao, K. N. Anuradha, S. Sarangi, and S. V. Bhat, Appl. Phys. Lett. **87**, 182503 (2005).
[39] Y. Wang and H. J. Fan, Appl. Phys. Lett. **98**, 142502 (2011).
[40] S. Dong, F. Gao, Z. Q. Wang, J. M. Liu, and Z. F. Ren, Appl. Phys. Lett. **90**, 082508 (2007).
[41] S. Dong, R. Yu, S. Yunoki, J. M. Liu, and E. Dagotto, Phys. Rev. B **78**, 064414 (2008).
[42] R. Maezono, S. Ishihara, and N. Nagaosa, Phys. Rev. B **58**, 11583 (1998).